Airborne Viral Emission and Risk Assessment in Enclosed Rooms

Mitul Luhar*
Department of Aerospace and Mechanical Engineering, USC

Note: This manuscript describes a simple model designed to assess airborne transmission risk for COVID-19 in enclosed rooms. There is significant variability in respiratory emissions of SARS-CoV-2 and the dose-response curve for COVID-19 is not well established, and so any quantitative guidelines presented in this document must be treated with caution. This work is preliminary and not peer-reviewed. For the interested reader, the following links provide some very useful additional information on airborne transmission of SARS-CoV-2 put together by a group of scientists and engineers with expertise related to indoor air quality, aerosol science, aerosol disease transmission, and engineered control systems for aerosols.

`https://tinyurl.com/FAQ-aerosols`
`https://tinyurl.com/covid-estimator`

1 Introduction

Transmission of the SARS-CoV-2 virus via larger respiratory droplets and direct contact with infected persons or contaminated surfaces has been established. However, there is increasing evidence to suggest that airborne transmission may be an important third route of infection [2, 5, 11, 18]. Airborne transmission is defined as transmission via inhalation of aerosols that can remain suspended for a long time. A size threshold of 5 μm is generally used to differentiate between airborne and droplet transmission ([35]; *n.b.,* this threshold seems a little arbitrary). Aerosols also include droplet nuclei which are produced through the process of rapid desiccation of exhaled respiratory droplets [28]. Existing spatial distancing, face covering, and hand hygiene guidelines are primarily concerned with limiting transmission via larger droplets and direct contact. However, even with these precautionary measures, airborne transmission may be important in enclosed spaces with a large number of occupants and over extended periods of contact (e.g., in classrooms, offices, places of worship, bars, restaurants, entertainment venues, airplane cabins, buses). Reports from China, Singapore and Nebraska have found low concentrations of airborne SARS-CoV-2 virus in hospital rooms and ventilation systems where COVID-19 patients have been treated [3, 13, 25]. Other studies have shown that infectious individuals at a call center and a choir practice—scenarios characterized by extensive vocalization—led to widespread transmission [9, 22]. Despite the mounting evidence for airborne transmission, there are few engineering guidelines on allowable contact duration and occupant density in enclosed spaces.

This document presents a simple model for airborne virus emission and exposure in an enclosed space. The goal is to provide an *estimate* for airborne virus concentrations and dosage for a known number of occupants and duration of contact. This will depend on the number of infectious persons in the room, whether the occupants are being active or passive, as well as any mitigating factors such as the use of face coverings, enhanced HVAC protocols, and limited occupant density due to spatial distancing. As illustrated in figure 1, the model assumes perfectly-mixed conditions in the room, such that the concentration of virus particles is uniform. In simple terms, the model assumes that any airborne particles are mixed throughout the space quickly. This assumption also implies a uniform transmission risk for all occupants in the room. Such *mixed flow* or *continuously-stirred reactor* models are common in indoor air quality modeling [e.g., 19, 20]. In the context of airborne disease transmission, such models are typically referred to as Wells-Riley models after pioneering studies in this field [23, 27, 32]. Recent efforts have also used such models to calculate SARS-CoV-2 airborne transmission risks for specific commercial interactions or case studies [2, 16]. We recognize that the perfectly-mixed assumption is a significant oversimplification since virus concentrations will be higher closer to the source of emission (i.e., an infectious person) and in the air jet created by talking

*luhar@usc.edu

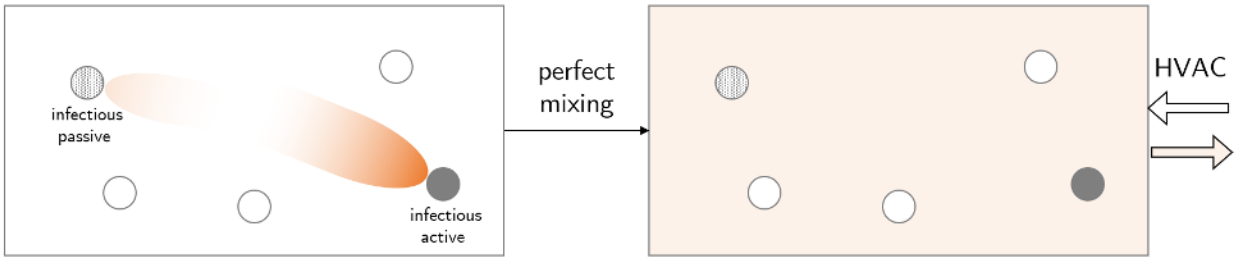

Figure 1: Schematic illustrating well-mixed room model. The room has N people, a fraction of which are infectious. Infectious persons are classified as either being active (e.g., talking loudly or lecturing) or passive (e.g., listening quietly). Respiratory virus emissions from the infectious persons are assumed to be mixed uniformly throughout the room. The ventilation system is assumed to bring in virus-free air.

or vocalization. Prevailing air currents from HVAC systems and any open doors or windows can also lead to localized hotspots. In other words some occupants in the room will be subject to higher exposure than that predicted by the model and others will be subject to lower exposure. Nevertheless, an increase in the exposure predicted by the model should be considered indicative of higher transmission risk overall. Higher-fidelity computational fluid dynamics simulations and/or experiments that capture the intricacies of droplet and aerosol transport from respiratory emissions in the presence of background air flow should be pursued wherever possible [see e.g., 30]. However, since running such complex simulations or experiments is not feasible for all potential scenarios, this model provides useful first-order estimates of airborne transmission risk in enclosed spaces.

The model is developed in §2. We use this model to provide general recommendations and consider specific scenarios in §3. We emphasize that this model does not consider transmission via larger respiratory droplets or direct contact, which are established pathways that current spatial distancing, PPE, and hand hygiene guidelines aim to address.

2 Model Development

2.1 Virus Concentration in Room and Dosage

Consider a room scale mass balance for virus concentration C (RNA copies m^{-3}) assuming perfectly-mixed conditions. The room has floor area A (m^2), height h (m), and volume $V = Ah$ (m^3). The volumetric flow rate through the HVAC system is Q_{hvac} ($\mathrm{m}^3\mathrm{s}^{-1}$) and the air exchange rate is $E_{hvac} = Q_{hvac}/V$ (s^{-1}). The total number of people in the room is N. The number of people per unit area is therefore $n = N/A$ (m^{-2}); this parameter will be impacted by any spatial distancing guidelines implemented. Each person is assumed to inspire and expire air at a volumetric rate of Q ($\mathrm{m}^3\mathrm{s}^{-1}$) on average, which can be estimated as the product of the tidal volume and breathing rate. The fraction of people in the room that are infectious is assumed to be p_i and so the total number of infectious persons in the room expected to be $N_i = p_i N$. The virus concentration in the expired air for an infected person is C_i^a if the person is being *active* (e.g., talking or lecturing loudly) and C_i^p if the person is being *passive* (e.g., listening quietly). The probability that an infectious person is active at any given time is p_a. The probability that an infectious person is passive is $p_p = 1 - p_a$. We can further assume that everyone is wearing a face covering and the filtration efficiency at expiration for active and passive persons is f^a and f^p respectively. The average settling velocity of the airborne particles is assumed to be v_s. Diffusive fluxes to surfaces are neglected, as is the decay in the number of viable or infectious virus particles over time. This latter assumption is made because there is still significant uncertainty regarding how long SARS-CoV-2 remains viable in aerosols or droplet nuclei [29].

With these assumptions, the virus concentration as a function of time (t) can be calculated using:

$$V\frac{dC}{dt} = Np_ip_a(1-f^a)C_i^aQ + Np_i(1-p_a)(1-f^p)C_i^pQ - NQC - Q_{hvac}C - Av_sC. \tag{1}$$

The first two terms on the right-hand side represent the source terms from active and passive persons in the

room while the last three terms represent sink terms due to inhalation by the occupants, HVAC air exchange, and settling onto surfaces. Note that the volumetric flow rate through the HVAC system is only considered a sink in the model, i.e., the model assumes that all the air flow into the room from the HVAC system is virus-free. This either requires a continuous supply of fresh air or effective in-line filtration. Dividing through by V, we have

$$\frac{dC}{dt} = \frac{NQ}{V}\left(p_i p_a (1-f^a) C_i^a + p_i(1-p_a)(1-f^p)C_i^p\right) - \left(\frac{NQ}{V} + \frac{Q_{hvac}}{V} + \frac{Av_s}{V}\right) C \tag{2}$$

or equivalently

$$\frac{dC}{dt} = \frac{nQ}{h}\left(p_i p_a (1-f^a) C_i^a + p_i(1-p_a)(1-f^p)C_i^p\right) - \left(\frac{nQ}{h} + E_{hvac} + \frac{v_s}{h}\right) C. \tag{3}$$

For steady-state conditions ($dC/dt = 0$), the virus concentration in the room is expected to be

$$C_{ss} = \frac{\frac{nQ}{h}\left(p_i p_a (1-f^a) C_i^a + p_i(1-p_a)(1-f^p)C_i^p\right)}{\left(\frac{nQ}{h} + E_{hvac} + \frac{v_s}{h}\right)}. \tag{4}$$

The transient solution to (3) can be computed analytically and expressed as:

$$C = C_{ss}\left[1 - \exp\left(-\left(\frac{nQ}{h} + E_{hvac} + \frac{v_s}{h}\right) t\right)\right]. \tag{5}$$

The virus intake rate I (RNA copies s^{-1}) for an individual can be estimated using (5) as

$$I = (1-\hat{f})CQ, \tag{6}$$

where $\hat{f}$ is the filtration efficiency due to any facial covering for inhaled particles. The virus dose D (RNA copies) over a contact duration T (s) is therefore expected to be

$$D = \int_0^T (1-\hat{f})CQdt. \tag{7}$$

For the expression shown in (5), this can be evaluated analytically to yield:

$$D = (1-\hat{f})QC_{ss}\left[T - \frac{1}{\left(\frac{nQ}{h} + E_{hvac} + \frac{v_s}{h}\right)}\left(1 - \exp\left(-\left(\frac{nQ}{h} + E_{hvac} + \frac{v_s}{h}\right) t\right)\right)\right]. \tag{8}$$

2.2 Time Scales and Model Simplification

Equations (5) and (8) show that there are three key rate constants (i.e., inverse time scales) involved in this problem. The first is set by the respiration-driven exchange, nQ/h (s^{-1}), the second depends on the HVAC air exchange E_{hvac} (s^{-1}), and the third depends on settling v_s/h (s^{-1}).

Assuming that the 6 ft (2 m) spatial distancing guidelines are being followed, we expect an occupant density of $n \approx 1/(2\,\mathrm{m})^2 \approx 0.25$ m^{-2}. For resting conditions, typical volumetric exchange rates due to breathing for an individual are $Q \approx 0.8 - 1.3 \times 10^{-4}$ m^3 s^{-1} (5-8 L min^{-1} [6]). However, this can rise to $Q \approx 0.6 - 1.0 \times 10^{-3}$ m^3 s^{-1} for moderate exercise. Assuming a typical room height of $h \approx 2.5$m (8 ft), for resting conditions we expect the following approximate range for the respiration-driven exchange rate

$$\frac{nQ}{h} \approx 8 \times 10^{-6} - 1.3 \times 10^{-5}\ \mathrm{s}^{-1}, \tag{9}$$

though this could rise by an order of magnitude in case of moderate exercise.

HVAC flow rates are typically specified in terms of the number of room volume changes per hour (c.f., $E_{hvac} = Q_{hvac}/V$) or as minimum ventilation rates per person. For low-traffic areas, rule-of-thumb guidelines

suggest 3-5 changes per hour. For busy areas with potential for poor air quality (e.g., kitchens, restrooms, parking garages) as many as 20-30 changes per hour are recommended [33]. Assuming a range of 4-12 changes per hour, we have the following range for HVAC air exchange rates

$$E_{hvac} \approx 1.1 \times 10^{-3} - 3.3 \times 10^{-3} \text{ s}^{-1}. \tag{10}$$

The average settling velocity of the aerosol particles depends strongly on particle size. The terminal settling speed for a spherical particle of diameter d and density ρ settling in air (with density $\rho_a = 1.2$ kg m^{-3} and viscosity $\mu_a = 1.8 \times 10^{-5}$ kg m^{-1}s^{-1}) can be estimated from Stokes' law as

$$v_s = \frac{(\rho - \rho_a) g d^2}{18 \mu_a}, \tag{11}$$

where $g = 9.81$ m s^{-2} is the acceleration due to gravity. Estimating an *average* settling velocity for the airborne particles is tricky since human emissions from breathing, talking etc., create a range of particle sizes [8]. Particle sizes also decrease over time due to vaporization, which depends on temperature, relative humidity, and the exact chemical composition [12]. Since the present study aims to evaluate airborne transmission, we can obtain an upper bound estimate for the average settling speed of aerosol particles by assuming a diameter of $d = 5\mu$m. For a lower bound estimate, we assume a particle diameter comparable to the size of the SARS-CoV-2 virus, $d \approx 0.12\mu$m [31]. Further assuming that the density of the particles is comparable to that of water, $\rho \approx 1000$ kg m^{-3}, we expect settling velocities $v_s \approx 4.4 \times 10^{-7}$ to 7.6×10^{-4} ms^{-1}. This translates into the following range for the settling rate constant

$$\frac{v_s}{h} \approx 1.8 \times 10^{-7} - 3.0 \times 10^{-4} \text{ s}^{-1}. \tag{12}$$

For particles with diameter smaller than $d \approx 10\mu$m, the Stokes' settling velocity in (11) is known to be an underestimate and must be modified using the so-called Cunningham correction factor [4]. For simplicity, we neglect this correction in the present analysis. In any case, a lower settling velocity will yield a conservative (higher) estimate for average virus concentration per (4).

A comparison of (9), (10), and (12) shows that the rate constant due to HVAC is an order of magnitude (or more) higher than the other two, $E_{hvac} \gg nQ/h$ and $E_{hvac} \gg v_s/h$. In other words, air exchange through the HVAC system is the most important *sink* for airborne particles that potentially contain virus. Settling and person-driven intake due to respiration are less important.

For HVAC-dominated exchange, the additional terms in (4) and (5) arising from settling and respiratory intake can be neglected, and it can be shown that (4) and (5) simplify to:

$$C_{ss} \approx \frac{nQ}{hE_{hvac}} p_i \left(p_a(1 - f^a) + (1 - p_a)(1 - f^p) \frac{C_i^p}{C_i^a} \right) C_i^a, \tag{13}$$

and

$$C \approx C_{ss} \left[1 - \exp\left(-E_{hvac} t \right) \right]. \tag{14}$$

Note that neglecting the additional parameters nQ/h and v_s/h in the denominator in (4) yields a conservative estimate for the steady state-concentration in (13). Equation (14) shows that the transient dynamics are primarily controlled by E_{hvac} and so we can estimate the time to steady state as $t_{ss} \approx 1/E_{hvac} \approx 900$ s (15 min) for the lowest air change rate and $t_{ss} \approx 300$ s (5 min) for the highest air change rate. Since we are primarily concerned with extended activities that are much longer than this time frame, we can assume steady-state conditions to estimate virus intake, yielding

$$D \approx (1 - \hat{f}) Q C_{ss} T. \tag{15}$$

Again, assuming steady-state conditions yields a conservative estimate for average dosage. Combining (13) and (15), we have:

$$D \approx (1 - \hat{f})(1 - f) \frac{nQ}{hE_{hvac}} p_i \left(p_a + (1 - p_a) \frac{C_i^p}{C_i^a} \right) Q C_i^a T, \tag{16}$$

where we have also assumed for simplicity that the filtration efficiencies at expiration for active and passive activities are identical $f = f^a = f^p$. Given the differing particle size distributions associated with breathing

Expiratory Activity	$d_1(0.8\mu\text{m})$	$d_2(1.8\mu\text{m})$	$d_3(3.5\mu\text{m})$	$d_4(5.5\mu\text{m})$
Speaking	0.751	0.139	0.139	0.059
Breathing	0.084	0.009	0.003	0.002

Table 1: Particle concentrations c_{dj} (cm^{-3}) of the different size distribution channels for speaking and breathing as measured by Morawska et al. [17]. Table modified from Buonanno et al. [2].

and talking [17] and the variation in mask filtration efficiency with particle size [10], this assumption should be revisited as specific scenarios are considered (i.e., different mask materials). The expressions shown in (13) and (16) lead to the following key observations:

- Steady state concentrations and dosage depend linearly on the density of people in the room n. This is because a higher occupant density also implies a higher number of potentially infectious people in the space. Recall that spatial distancing guidelines come in via this term.
- Increased HVAC air change rates (E_{hvac}) lead to a reduction in steady state concentrations. This is because higher flow rates through the HVAC system lead to faster removal of aerosols that are potentially virus laden.
- Virus intake increases linearly with the duration of exposure T.
- The virus dose depends strongly on the filtration efficiency of the masks. The effects of inward protection ($\hat{f}$) and outward protection (f) are compounded. Note that filtration efficiencies vary as a function of particle size [10]. The factors used here (f) and ($\hat{f}$) are integrated measures.

It is important to keep in mind this model assumes that the HVAC systems serve purely as a sink, i.e., virus concentration in the air being fed in to the room is zero. This requires a continuous input of fresh air or effective in-line filtration if the air is being recirculated. It remains to be seen if this assumption is realistic for installed HVAC systems.

To proceed, additional information is needed. Filtration efficiencies for a variety of surgical and cloth face coverings can be found in Konda et al. [10]. With proper sealing, filtration efficiencies are over 90% though the presence of any gaps can bring this down to roughly 50%. The fraction of people that are infectious (p_i) can be estimated from LA-county wide data, though the presence of a local "hotspot" could lead to higher values for p_i. Given the likely spread in these parameters, we can potentially use a Monte Carlo approach to generate statistical outputs. Estimates for airborne virus emission rates are provided in the following section. We use (16) to make general recommendations and consider specific scenarios in §3.

2.3 Virus Emission Rates

The emission rates C_i^a and C_i^p can be estimated based on known virus concentrations and aerosol volumes for typical active and passive activities [1, 2, 26]. For instance, Stadnytskyi et al. [26] suggest that 25 s of active or loud speaking leads to the emission of between 60 and 320 nL of oral fluid. The viral load in the sputum is estimated to be $c_v \approx 7 \times 10^6$ RNA copies cm^{-3}, though this may be as high as $\text{O}(10^9)$ RNA copies cm^{-3} [34]. Based on these estimates, the virus output for an active infected person is expected to range from $QC_i^a \approx \frac{60\times10^{-6}\cdot7\times10^6}{25} \approx 17$ RNA copies s^{-1} to $QC_i^a \approx \frac{320\times10^{-6}\cdot7\times10^6}{25} \approx 90$ RNA copies s^{-1}.

Alternate estimates for virus emission can be obtained following the approach of Buonanno et al. [2] based on the particle size and density distributions provided by Morawska et al. [17]. If the number concentration of particles c_{dj} (m^{-3}) of a given diameter d_j (m) is known for the activity being considered, the virus output can be estimated as

$$QC_i \approx Qc_v \sum_j c_{dj} \frac{\pi}{6} d_j^3. \tag{17}$$

Based on the data provided in Table 1, and assuming $Q \approx 10^{-4}$ m^3s^{-1} and $c_v \approx 7 \times 10^6$ RNA copies cm^{-3} as before, the virus output is estimated to be $QC_i^a \approx 6 \times 10^{-3}$ RNA copies s^{-1} for active (i.e., speaking) persons and $QC_i^p \approx 2 \times 10^{-4}$ RNA copies s^{-1} for passive (i.e., resting) persons. Thus, the virus emission rate is expected to be roughly *40 times higher* for active persons relative to passive persons. In other words, we

expect $(C_i^p/C_i^a) \approx 0.025$ in (16). This indicates that the cumulative emissions from the passive fraction only become comparable to the emissions from the active fraction for very low activity levels, $p_a \lesssim 0.025$. For higher activity levels ($p_a \gtrsim 0.25$), active emissions are an order of magnitude higher than passive emissions and (16) can be simplified further to:

$$D \approx (1-\hat{f})(1-f)\frac{nQ}{hE_{hvac}} p_i p_a Q C_i^a T. \tag{18}$$

Note that the active virus emission rate, QC_i^a, estimated following the approach of Buonanno et al. [2] is three orders of magnitude lower than the estimate based on the data reported in Stadnytskyi et al. [26]. This discrepancy could be explained by the fact that volumetric emission rates reported by Stadnytskyi et al. [26] are corrected for dehydration. Indeed, size estimates for the droplet nuclei at the point of measurement in Stadnytskyi et al. [26], $d \approx 4\mu$m, are in reasonable agreement with the size distributions measured by Morawska et al. [17] during speech. However, Stadnytskyi et al. [26] use estimates for the hydrated particle diameter ($d \approx 12-21\mu$m) to calculate volumetric emissions. Since the emission rate scales as d^3, a factor-5 difference in diameter between hydrated and measured diameter could explain much of the discrepancy in QC_i^a. Buonanno et al. [2] also suggest a slightly higher range of values for viral load, $c_v \approx 10^8 - 10^{10}$ RNA copies cm^{-3} [21, 24].

In summary, there is a wide range of viral loads (c_v) reported in previous literature [21, 24, 34]. The technical challenges inherent in estimating particle diameters and emission volumes associated with active and passive activities [8] further complicate assessment of virus emission rates. To generate preliminary *quantitative* assessments of airborne transmission risk, we consider the conservative (higher) emission rates suggested by Stadnytskyi et al. [26]. Specifically, we assume that SARS-CoV-2 emission rates for active persons are in the range $QC_i^a \approx 17-90$ RNA copies s^{-1}. We assume that emission rates for passive persons are a factor of 40 lower, $QC_i^p \approx 0.5-2$ RNA copies s^{-1} [2]. The minimum infectious dose for COVID-19 is still unknown but estimates quoted in the media suggest that it could be as low as several hundred RNA copies [7]. In general, the severity of symptoms is also thought to be linked to the amount of exposure [36]. To translate the virus dosage estimates into a transmission probability p_t, we can use a function of the form

$$p_t = 1 - \exp\left(-\frac{D}{D_i}\right), \tag{19}$$

where D_i is the dose that leads to transmission in roughly 63% of cases [2, 23]. Note that the exponential mapping used to translate virus dose into a transmission probability implicitly accounts for the variation in physiological responses to the same exposure as well as the room-scale variation in exposure that the well-mixed model neglects (i.e., arising from concentration hotspots). If the infectious dose is $D_i = 1000$ RNA copies, the respiratory emission estimates provided above suggest that active infectious persons can emit roughly 60 to 320 infectious doses per hour while passive persons can emit roughly 1.8 to 7 infectious doses per hour. These estimates are consistent with the predictions made by Buonanno et al. [2], who suggest that asymptomatic infectious persons undergoing light activity and talking can generate over 100 quanta per hour, where a quantum is defined as the dose of airborne droplet nuclei required to cause infection in 63% of susceptible persons.

Given the wide range in expected viral emission rates and the substantial simplifications inherent in the well-mixed room model (e.g., neglecting the effect of concentration hotspots), we suggest that a predicted virus intake of $D = 100$ RNA copies for the parameters assumed in this document should be considered dangerous, though doses below this value could also lead to transmission. For $D_i = 1000$ RNA copies, an intake of $D = 100$ RNA copies implies $p_t \approx 0.1$, i.e., a 10% transmission risk. Finally, for a given transmission probability, the number of expected transmissions can be estimated as $N_t \approx p_t N$.

3 Model Predictions and Recommendations

In this section, we generate quantitative estimates for airborne concentrations, virus doses, and transmission probabilities using the expressions shown in (13), (16) or (18), and (19). Typical values for the various terms appearing in these equations are listed in Table 2. We first consider a few specific case studies (§3.1) and university-relevant scenarios (§3.2) before pursuing a parametric study (§3.3) that evaluates the effect of facial coverings, probability of infection and activity, occupant spatial density, and HVAC air change rates.

Respiration rate, Q	10^{-4} m^{3}s^{-1} (6 L min^{-1})
Occupant density, n	0.25 m^{-2}
Room height, h	2.5 m
HVAC air change rate, E_{hvac}	1.1×10^{-3} s^{-1} (4 hr^{-1})
Active emission rate, QC_i^a	40 RNA copies s^{-1}
Passive-active emission ratio, C_i^p/C_i^a	1/40
Mask filtration efficiency, $f = \hat{f}$	0.5
Active fraction, p_a	0.1
Duration of exposure, T	3600 s
Infectious Dose, D_i	1000 RNA Copies

Table 2: Assumed parameter values (unless otherwise specified).

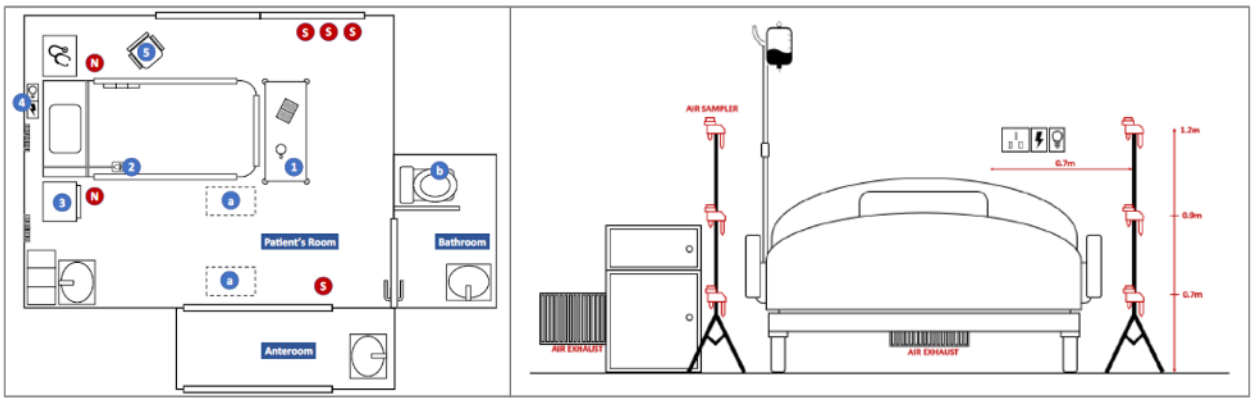

Figure 2: Schematic showing location of air sampling units (red circles marked with an N) in AIIRs where measurements show presence of airborne SARS-CoV-2; modified from Chia et al. [3].

3.1 Real-world Measurements and Suspected Airborne Transmission Events

In this section, we compare model predictions against measurements of airborne SARS-CoV-2 in hospitals [3] and real-world events in which airborne transmission is suspected [9, 11, 22]. Note that transmission via respiratory droplets and contact with contaminated surfaces is still likely in the case studies considered below; airborne transmission is another potential pathway.

3.1.1 Airborne SARS-CoV-2 at National Center for Infectious Diseases, Singapore

Recent measurements by Chia et al. [3] have shown the presence of aerosolized SARS-CoV-2 in airborne infection isolation rooms (AIIRs) at the National Center of Infectious Diseases in Singapore. Chia et al. [3] collected air samples over a period of 4 hours in three different AIIRs, and subsequently analyzed these samples for the presence of SARS-CoV-2 RNA. Measured airborne concentrations of SARS-CoV-2 ranged from 1.84×10^3 to 3.38×10^3 RNA copies per m^3 of sampled air in two AIIRs occupied by patients on Day 5 of illness. Airborne SARS-CoV-2 was not detected in an AIIR occupied by a patient on Day 9 of illness.

The report by Chia et al. [3] suggests that the AIIRs were characterized by high air change rates, $E_{hvac} = 3.3 \times 10^{-3}$ s^{-1} (12 changes hr^{-1}). The exhaust flow rate was reported to be 580 m^{3}hr^{-1}. With 12 air changes per hour, this exhaust flow rate suggests a room volume of $V = 580/12 \approx 48$ m^3. Assuming one infectious occupant in each AIIR, we have $n/h = 1/48$ m^{-3} and $p_i = 1$. Further, since all patients were reported to be symptomatic, we assume a high activity level, $p_a = 1$. With these parameters, (13) suggests an average steady state concentration of $C_{ss} \approx 250$ RNA copies m^{-3}. This prediction for steady-state concentration is an order of magnitude lower than the airborne concentrations measured by Chia et al. [3]. This discrepancy could be attributed to a number of reasons. First, the air sampling units were placed very close to the bed of the patient and the exhaust vent (see figure 2). As such, the measured concentrations are expected to be higher than the *average* concentrations in the room predicted by the

well-mixed model. Second, the viral load in respiratory emissions from the patients may have been higher than the range estimated in the previous section ($17 - 90$ RNA copies s^{-1} for active vocalization). For reference, the predicted value of $C_{ss} \approx 250$ RNA copies m^{-3} assumed an emission rate of $QC_i^a = 40$ RNA copies s^{-1}. For an emission rate at the upper end of the estimated range, $QC_i^a = 90$ RNA copies s^{-1}, the predicted steady state concentration increases to $C_{ss} \approx 560$ RNA copies m^{-3}, which is within a factor 3 to 6 of the measurements. However, given the wide range of reported viral loads in oral fluid [2, 26], even this higher emission rate may be an underestimate, especially for symptomatic patients that are coughing or experiencing difficulty breathing.

Despite the quantitative discrepancy between predicted steady-state concentrations and airborne concentrations of SARS-CoV-2 measured by Chia et al. [3], the discussion above highlights the utility of the well-mixed room model in generating preliminary estimates of airborne virus concentrations and transmission risk. Below, we use the model to consider specific events in which airborne transmission is suspected.

3.1.2 Case Study: Choir Practice in Skagit County, WA

Next, we consider the choir practice that took place in Skagit County (WA) in March that has been widely reported as a super-spreader event [9, 16]. A recent case study by Miller et al. [16] provides an in-depth analysis of this event.

Following a 2.5-hour choir practice attended by 61 persons, including a symptomatic individual, 32 confirmed and 20 probable secondary COVID-19 cases occurred. The case report by Hamner [9] suggests that transmission was facilitated by proximity (less than 6 feet) during practice and augmented by the act of singing. Since this event took place prior to widespread adoption of current guidelines on spatial distancing and facial coverings, transmission via the established droplet and direct contact pathways is likely. Nevertheless, given the high rate of infection (up to 52 out of 61 people, or 85%), it is possible that airborne transmission occurred as well. We evaluate this scenario below.

To represent this event, we assume an exposure time of $T = 9000$ s (2.5 hours) and an infectious fraction of $p_i = 1/61$. Since singing is known to produce airborne particles at much higher rates than talking [1, 14], we assume that the choir practice was characterized by continuous activity ($p_a = 1$). We also assume the absence of any face coverings ($f = \hat{f} = 0$). The case report suggests that the attendees sat in chairs separated by 6 to 10 inches (0.25 m) and roughly 1 in 2 chairs were occupied. Based on this information, we assume an average separation of 1 m or roughly 3 ft between attendees (separated by a chair and 6-10 inches on either side). This translates into a spatial density of $n \approx 1$ m^{-2}. Finally, ventilation estimates for the practice space suggest relatively low air change rates of less than 1 turnover per hour, i.e., $E_{hvac} \leq 2.7 \times 10^{-4}$ s^{-1}. The predictions below assume $E_{hvac} = 2.7 \times 10^{-4}$ s^{-1}. For these high-occupancy, high-activity, and low-ventilation conditions, (18) suggests an expected SARS-CoV-2 intake of

$$D \approx \frac{nQ}{hE_{hvac}} p_i p_a Q C_i^a T \approx 910 \text{ RNA copies.} \tag{20}$$

For an infectious dose of $D_i = 1000$ RNA copies, this would translate into an expected transmission rate of $p_t \approx 0.60$ or 60%. In a very rough sense, this is consistent with the observed transmission rate of up to 85%, especially given the likelihood of droplet or direct contact transmission. The high predicted dose, coupled with the high SARS-CoV-2 attack rate observed at the choir practice, suggests that airborne transmission could have been a third transmission pathway at the choir practice. At the very least, this case study suggests that a predicted dose of 910 RNA copies under the model developed here should be considered indicative of very high transmission risk.

3.1.3 Case Study: Call Center in Seoul, South Korea

Transmission via aerosols is also suspected in the COVID-19 outbreak that took place in late February and early March in a call center in South Korea. The case report by Park et al. [22] indicates that a single employee may have infected 94 of 216 employees working on the same floor over the course of a week; an attack rate of 43.5%. The spatial distribution of the cases shown in figure 3 indicates transmission beyond the nearest neighbor to the infectious person. The case report indicates no shared dining area, though it is possible that close interactions beyond immediate neighbors in the floor plan could have occurred in restrooms, elevators,

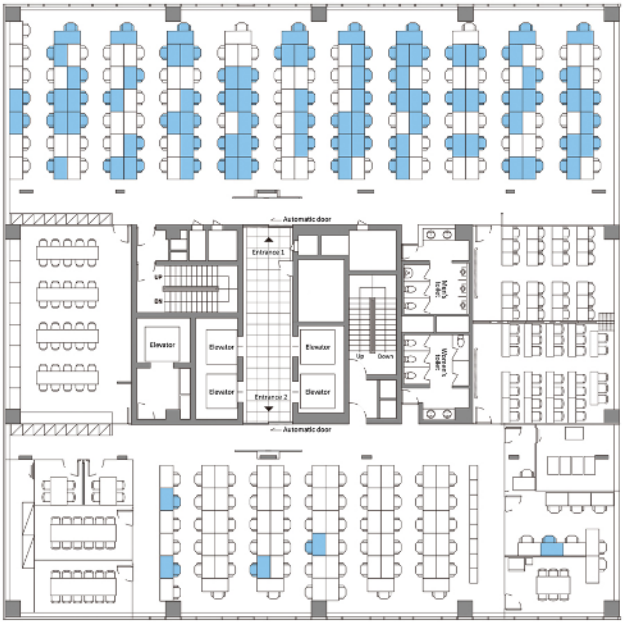

Figure 3: Floor layout and distribution of infected persons for the COVID-19 outbreak in a call center in South Korea; from Park et al. [22]. Seating positions for persons with confirmed infections are highlighted in blue.

etc. To analyze this case, we consider the open plan desk space towards the top of figure 3. This space housed 137 occupants, of which 79 (57.7%) contracted COVID-19. The floor area for this space is estimated from the schematic to be roughly 300 m^2, and so the occupant density is $n \approx 137/300 \approx 0.45\ \mathrm{m}^{-2}$. To generate model predictions for this case, we assume that 1 out of the 137 occupants was infectious initially ($p_i = 1/137$) and no masks were worn, and we consider a high activity rate consistent with call center tasks ($p_a = 0.75$). In the absence of more detailed information, we assume a room height of $h = 2.5$ m and an HVAC air change rate of $E_{hvac} = 1.1 \times 10^{-3}\ \mathrm{s}^{-1}$ (4 changes hr^{-1}). With these assumptions, the predicted virus dose over a typical 8 hour workday ($T = 28800$ s) can be estimated using (18) as:

$$D \approx \frac{nQ}{hE_{hvac}} p_i p_a Q C_i^a T \approx 100 \text{ RNA copies.} \tag{21}$$

For an infectious dose of $D_i = 1000$ RNA copies, this would translate into a transmission probability of just under 10%, $p_t \approx 0.098$. Assuming the transmission probability for each day is independent, over the course of a 5-day workweek, this would compound to a total transmission probability of roughly 40%. Again, this is broadly consistent with the observed attack rate of 57.7% in the open plan office space, bearing in mind that many of the infections may have occurred via droplet or direct contact transmission.

3.1.4 Case Study: Restaurant in Guangzhou, China

Another event that is indicative of partial airborne transmission is the case of the restaurant in Guangzhou, China. Reports published by Li et al. [11] and Lu et al. [15] show that an asymptomatic person dining at the restaurant (index patient A1 in figure 4) infected 9 others; 4 persons sitting at the same table and 5 persons at adjacent tables sitting more than 6 feet away. A detailed analysis carried out by Li et al. [11] suggests that the restaurant was crowded at the time of the event: there were $N = 83$ patrons distributed with an average area of 1.55 m^2 per person, i.e., $n \approx 0.65\ \mathrm{m}^{-2}$). Moreover, subsequent tracer gas studies showed that the restaurant was poorly ventilated with an air change rate between 0.56 and 0.77 changes hr^{-1}, which translates into $E_{hvac} \approx 1.5 \times 10^{-4}$ to $1.9 \times 10^{-4}\ \mathrm{s}^{-1}$. Assuming that transmission took place over roughly 1 hour ($T = 3600$ s), that no masks were worn, and that the meal was characterized by high

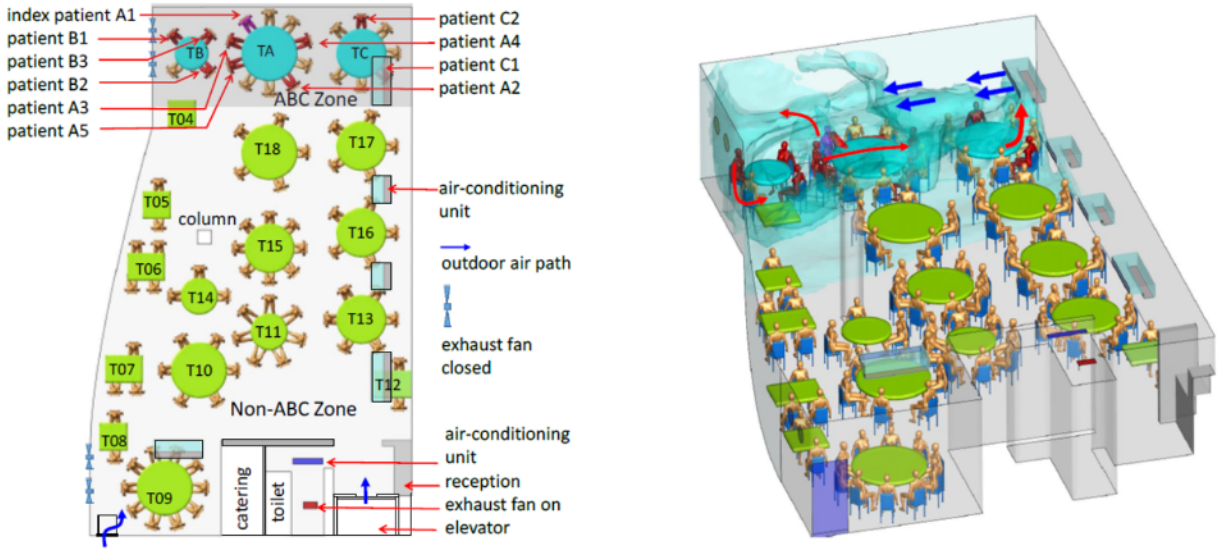

Figure 4: COVID-19 transmission at a restaurant in Guangzhou, China, including results from a CFD analysis. Confirmed infections are shown in red. Figures are reproduced from Li et al. [11].

activity levels, $p_a = 0.5$, the expression in (18) suggests an average dose of:

$$D \approx \frac{nQ}{hE_{hvac}} p_i p_a Q C_i^a T \approx 130 \text{ RNA copies} \tag{22}$$

for the restaurant as a whole, i.e., assuming that $p_i = 1/83$. For $D_i = 1000$ RNA copies, this translates into a transmission probability of $p_t \approx 0.12$ (12%). This is broadly consistent with 9 out of 83 patrons (10.8%) being infected, especially bearing in mind that not all patrons are likely to have been in the restaurant for the same duration of time.

The CFD visualization shown in figure 4 also suggests that a localized analysis for the ABC zone closest to the infectious person may be more appropriate, since the 3 tables in this zone were served by the same air conditioning unit. Figure 4 shows that these 3 tables had a total of 21 patrons. Considering just this zone leads to a higher infectious fraction, $p_i = 1/21$, and so the predicted dose increases to $D \approx 530$ RNA copies. For $D_i = 1000$ RNA copies as before, the transmission probability is $p_t \approx 0.4$ (40%). Again, this estimate is in line with 9 out of 21 patrons sitting in the ABC zone (42.9%) being infected.

3.2 University-Relevant Scenarios

The case studies considered in the previous section suggest that the well-mixed room model, with the parameter values listed in Table 2, yields useful results for steady state concentrations, virus doses, and transmission risk. In this section, we use the model to evaluate virus intake and transmission risk for two university-relevant scenarios: classrooms and research labs.

3.2.1 Case Study: Classrooms

Given the 40-fold difference between virus emission rates for passive and active persons, the worst-case scenario for a classroom setting would involve an *active* infectious lecturer. Per the discussion in §2.3, the cumulative emissions from the *passive* students would only become comparable to those from the lecturer if there were 40 times as many infectious students. This is unlikely. For this scenario involving an infectious lecturer, we have $p_i \approx 1/N$ where N is the number of occupants in the room and we assume that the instructor is active all of the time, $p_a = 1$. The ASHRAE-recommended air change rate for classrooms is 4

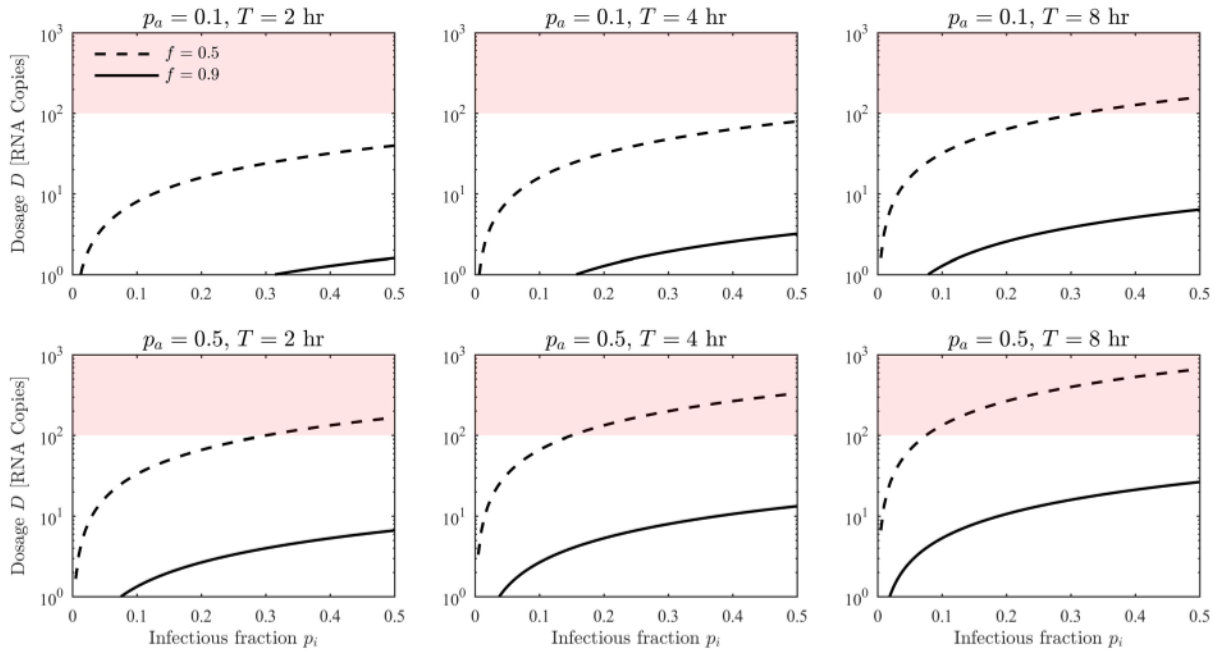

Figure 5: Figure showing predicted virus intake as a function of exposure time (T) under current research laboratory spatial distancing guidelines ($n \approx 0.1$ m^{-2}) assuming activity rates of $p_a = 0.1$ (top row) and $p_a = 0.5$ (bottom row). The remaining parameters are listed in Table 2.

changes hr^{-1}, or $E_{hvac} = 1.1 \times 10^{-3}$ s^{-1}. For these conditions, (18) can be simplified to:

$$D \approx (1-\hat{f})(1-f)\frac{nQ}{hE_{hvac}}\frac{1}{N}p_a Q C_i^a T = (1-\hat{f})(1-f)\frac{Q}{VE_{hvac}}p_a Q C_i^a T. \tag{23}$$

With the remaining parameters as specified in Table 2, this expression yields an expected dose of $D \approx \frac{320}{N}$ RNA copies. Thus, for larger classrooms capable of accommodating more than $N > 20$ students under the current (2 m) spatial distancing guidelines, $D < 20$ RNA copies and the model suggests a low risk of airborne transmission due to an infectious lecturer: $p_t < 0.02$ for $D_i = 1000$ RNA copies per (19). Keep in mind that, for larger classrooms, a low transmission probability could still translate into higher transmitted cases, $N_t \approx p_t N$. For smaller classrooms or seminar rooms that can only accommodate 2-3 occupants under the current spatial distancing guidelines, the predicted dosage from an infectious lecturer approaches $D \approx 100$ RNA copies and the risk of transmission increases. This dependence on the physical size of the classroom is made clearer by the second expression in (23), which shows that the virus dose is inversely proportional to room volume V. These predictions assume that all persons are wearing masks with inward and outward filtration efficiencies of $f = \hat{f} = 0.5$. Improved filtration efficiencies would further decrease risk. Keep in mind that the above estimates assume a class duration of $T = 1$ hr. The virus intake would increase with higher exposure times.

3.2.2 Case Study: Laboratories

Current USC guidelines suggest that research laboratories may be reoccupied so long as 10 ft (3 m) spacing is maintained, which translates into an upper limit on occupant density of $n \approx 0.1$ m^{-2}. Face coverings are also mandatory. The activity level in labs is expected to vary, depending on the type of research being conducted. In most cases, we anticipate relatively low activity in the labs with $p_a \leq 0.1$. However, labs requiring greater physical exertion or collaborative activities could require higher activity levels. We use $p_a = 0.5$ as an upper-bound activity estimate for such cases.

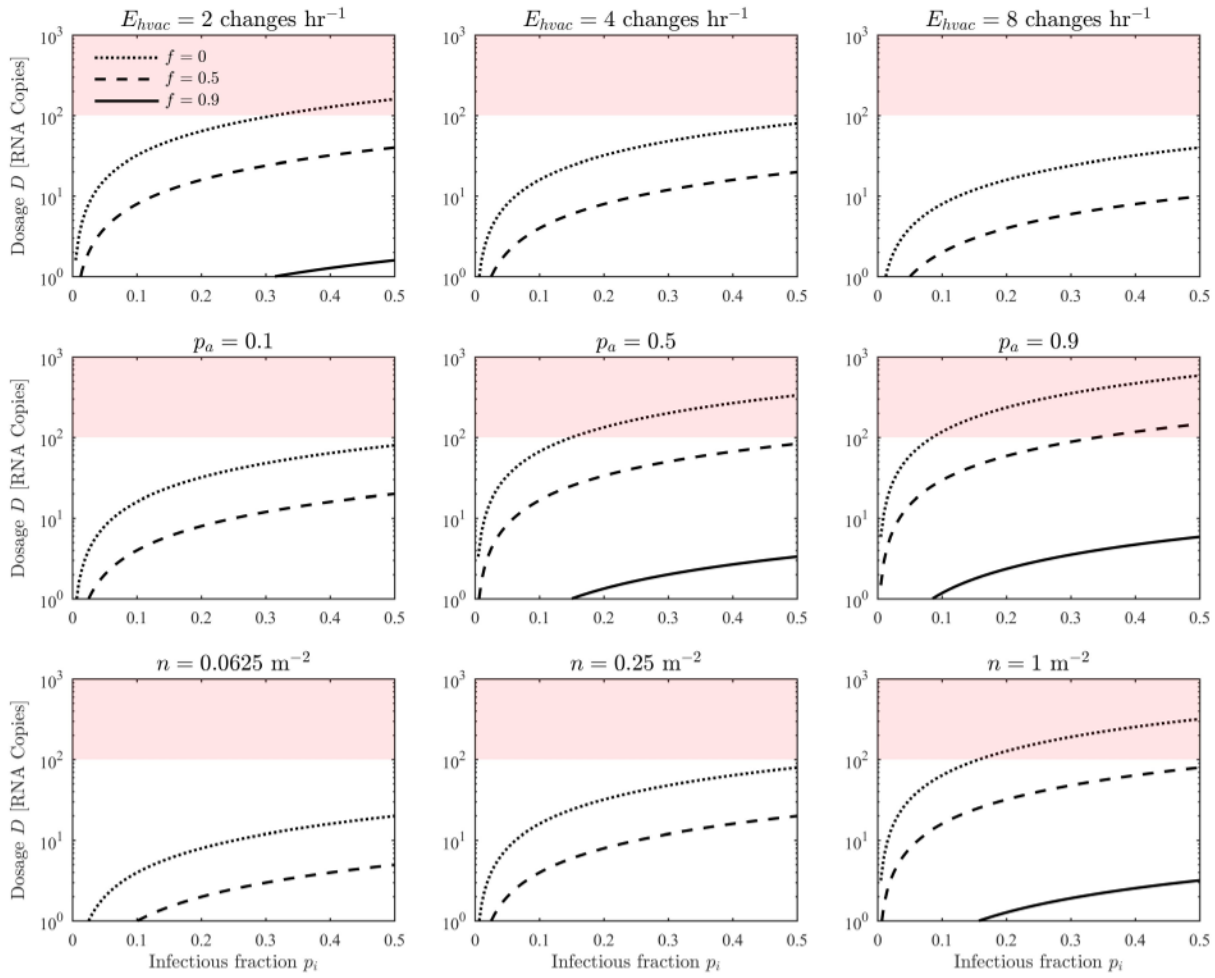

Figure 6: Predicted virus intake over 1 hours for a range of HVAC air change rates (top row), activity levels (middle row), and occupant spatial density (bottom row). In all plots, the dotted line shows predictions without masks ($f = \hat{f} = 0$) while the dashed and solid lines show predictions assuming 50% and 90% filtration efficiency. Assumed parameters are listed in Table 2 unless otherwise specified.

Figure 5 shows the virus dosage predicted using (16) for a range of exposure times for both low and high activity levels, $p_a = 0.1$ and $p_a = 0.5$. For typical labs with $p_a = 0.1$, exposure levels are not predicted to exceed $D \approx 100$ RNA copies except for cases compounded by long contact times (8 hr), 50% efficiency masks, and high infectious fractions $p_i > 0.3$, i.e., if 1 of 3 occupants in a small lab is infectious. The importance of effective face coverings is evident in the predictions for high-activity labs with $p_a = 0.5$. For this scenario, a mask filtration efficiency of 90% ($f = \hat{f} = 0.9$) keeps dosage well below 100 RNA copies. However, masks with filtration efficiencies of 50% could lead to exposures over this threshold for extended periods of contact, particularly for cases in which the infectious fraction is high, $p_i > 0.2$. This would be the case for smaller labs with 5 or less occupants in which 1 of the occupants is infectious.

3.3 Parametric Dependence

Finally, in this section, we pursue a parametric study of virus intake and transmission probability. Figure 6 shows representative results for virus intake over 1 hour as a function of HVAC air change rates (E_{hvac}), activity levels (p_a), and occupant spatial density (n). In general, these predictions emphasize the importance of wearing appropriate face coverings. Exposures only exceed $D > 100$ RNA copies (red shading in figure 6)

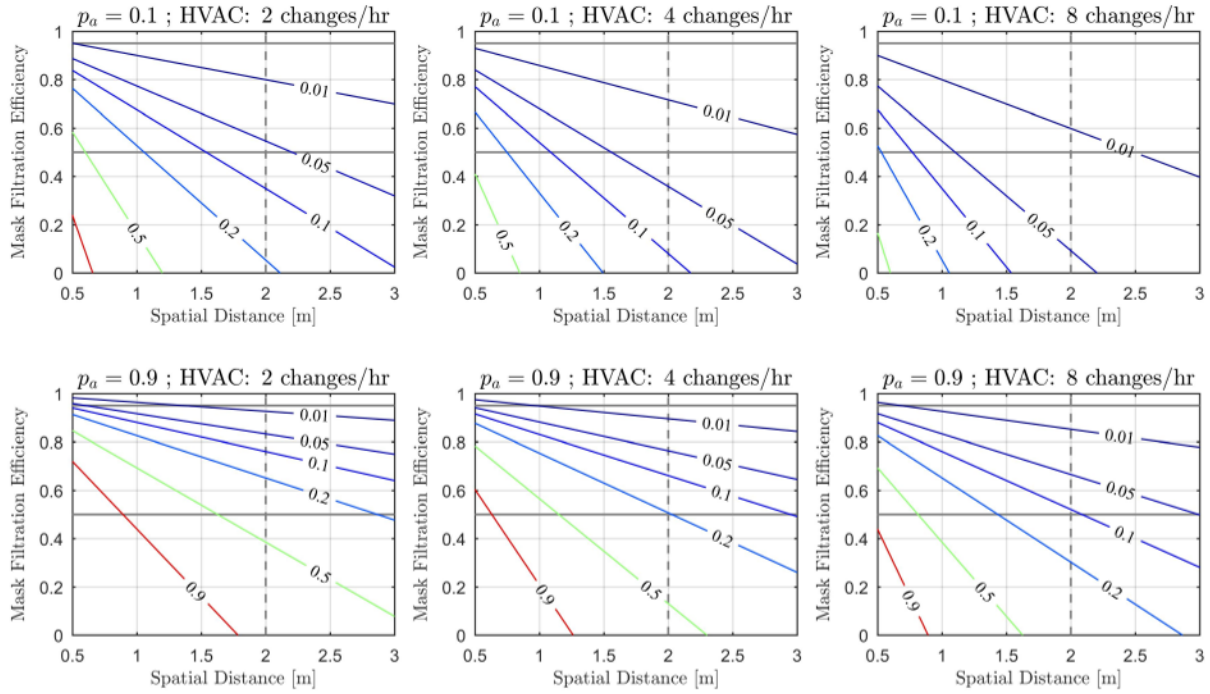

Figure 7: Transmission probabilities predicted using (19) as a function of mask filtration efficiency ($f = \hat{f}$) and average spatial distance ($n^{-1/2}$) between occupants in a room. These estimates assume that $p_i = 0.1$ (i.e., 1 in 10 occupants in the room is infectious) and an exposure time of $T = 28800$ s (8 hr). All other parameters not specified in the figure are listed in Table 2.

in the absence of filtration. As expected, a decrease in HVAC air exchange rates leads to increased risk, and increases in activity levels and occupant spatial density lead to increased risk. Keep in mind that although the predicted dose decreases as the occupant density decreases (bottom row in figure 6), the model still indicates a non-zero chance of airborne transmission when the average separation becomes larger than the current 6 ft (2 m) guidelines ($n < 0.25$ m^{-2}) due to the assumption that the virus-laden aerosols are mixed throughout the room. The perfect mixing assumption also implies that all individuals in the room are exposed to the same risk of airborne transmission. As noted earlier, this is an oversimplification (i.e., there will be spatial variations in airborne concentration; high concentrations near the infectious person and potential hotspots due to air currents). Nevertheless, this observation does highlight the possibility of airborne transmission beyond the current the 6 ft spatial distancing guidelines as well as the possibility of transmission beyond just the nearest neighbor.

The predictions shown in figure 6 assume an exposure time of 1 hour ($T = 3600$ s). Since the virus dose is expected to increase linearly with time (16), extended exposure times would lead to further increases in risk of airborne transmission. Figure 7 shows transmission probabilities predicted using (19) for an exposure time corresponding to a typical workday, $T = 8$ hr, assuming that 1 in 10 occupants in the room is infectious, $p_i = 0.1$. The top row shows predictions for a low-activity environment ($p_a = 0.1$) while the bottom row shows predictions for a high-activity environment ($p_a = 0.9$). The HVAC air change rates increase from left to right. These predictions show relatively low transmission risk ($p_t < 0.01$) if all occupants wear high-quality masks with $f = \hat{f} > 0.9$ and maintain the 6 ft (2 m) spatial distancing rules. However, if the occupants only have access to low-quality or ill-fitting masks with filtration efficiencies below 50%, $f = \hat{f} < 0.5$, even the 6 ft (2 m) spatial distancing rules may not be sufficient to prevent transmission, especially in poorly ventilated environments. These predictions suggest that for spaces such as open-plan offices or laboratories that are characterized by long-duration occupancy, more restrictive guidelines on spatial density may be

needed. Additional interventions such as improved ventilation, physical barriers, or limits on occupancy duration would also help in reducing the potential for airborne transmission.

Acknowledgements

Technical input and editorial feedback from colleagues at the Viterbi School of Engineering (Felipe De Barros, George Ban-Weiss, Ivan Bermejo-Moreno, Fokion Egolfopoulos, Paul Ronney, Neil Siegel, Assad Oberai, and Yannis Yortsos) and the Keck School of Medicine (Elisabeth Ference, Darryl Hwang, and Daniel Stemen) is gratefully acknowledged.

References

[1] S. Asadi, A. S. Wexler, C. D. Cappa, S. Barreda, N. M. Bouvier, and W. D. Ristenpart. Aerosol emission and superemission during human speech increase with voice loudness. *Scientific reports*, 9(1): 1–10, 2019.

[2] G. Buonanno, L. Stabile, and L. Morawska. Estimation of airborne viral emission: quanta emission rate of sars-cov-2 for infection risk assessment. *Environment International*, page 105794, 2020.

[3] P. Y. Chia, K. K. Coleman, Y. K. Tan, S. W. X. Ong, M. Gum, S. K. Lau, X. F. Lim, A. S. Lim, S. Sutjipto, P. H. Lee, et al. Detection of air and surface contamination by sars-cov-2 in hospital rooms of infected patients. *Nature communications*, 11(1):1–7, 2020.

[4] E. Cunningham. On the velocity of steady fall of spherical particles through fluid medium. *Proceedings of the Royal Society of London. Series A, Containing Papers of a Mathematical and Physical Character*, 83(563):357–365, 1910.

[5] S. J. Dancer, J. W. Tang, L. C. Marr, S. Miller, L. Morawska, and J. L. Jimenez. Putting a balance on the aerosolization debate around sars-cov-2. *Journal of Hospital Infection*, 2020.

[6] J. J. Feher. *Quantitative human physiology: an introduction*. Academic press, 2017.

[7] L. Geddes. Does a high viral load or infectious dose make COVID-19 worse?, 2020. URL `"https://www.newscientist.com/article/2238819-does-a-high-viral-load-or-infectious\ \-dose-make-covid-19-worse/"`. [Online; accessed 20-June-2020].

[8] J. Gralton, E. Tovey, M.-L. McLaws, and W. D. Rawlinson. The role of particle size in aerosolised pathogen transmission: a review. *Journal of Infection*, 62(1):1–13, 2011.

[9] L. Hamner. High sars-cov-2 attack rate following exposure at a choir practice—skagit county, washington, march 2020. *MMWR. Morbidity and Mortality Weekly Report*, 69, 2020.

[10] A. Konda, A. Prakash, G. A. Moss, M. Schmoldt, G. D. Grant, and S. Guha. Aerosol filtration efficiency of common fabrics used in respiratory cloth masks. *ACS nano*, 14(5):6339–6347, 2020.

[11] Y. Li, H. Qian, J. Hang, X. Chen, L. Hong, P. Liang, J. Li, S. Xiao, J. Wei, L. Liu, et al. Evidence for probable aerosol transmission of sars-cov-2 in a poorly ventilated restaurant. *medRxiv*, 2020.

[12] L. Liu, J. Wei, Y. Li, and A. Ooi. Evaporation and dispersion of respiratory droplets from coughing. *Indoor Air*, 27(1):179–190, 2017.

[13] Y. Liu, Z. Ning, Y. Chen, M. Guo, Y. Liu, N. K. Gali, L. Sun, Y. Duan, J. Cai, D. Westerdahl, et al. Aerodynamic analysis of sars-cov-2 in two wuhan hospitals. *Nature*, pages 1–4, 2020.

[14] R. G. Loudon and R. M. Roberts. Singing and the dissemination of tuberculosis. *American Review of Respiratory Disease*, 98(2):297–300, 1968.

[15] J. Lu, J. Gu, K. Li, C. Xu, W. Su, Z. Lai, D. Zhou, C. Yu, B. Xu, and Z. Yang. Covid-19 outbreak associated with air conditioning in restaurant, guangzhou, china, 2020. *Emerging infectious diseases*, 26(7):1628, 2020.

[16] S. L. Miller, W. W. Nazaroff, J. L. Jimenez, A. Boerstra, G. Buonanno, S. J. Dancer, J. Kurnitski, L. C. Marr, L. Morawska, and C. Noakes. Transmission of sars-cov-2 by inhalation of respiratory aerosol in the skagit valley chorale superspreading event. *medRxiv*, 2020.

[17] L. Morawska, G. Johnson, Z. Ristovski, M. Hargreaves, K. Mengersen, S. Corbett, C. Y. H. Chao, Y. Li, and D. Katoshevski. Size distribution and sites of origin of droplets expelled from the human respiratory tract during expiratory activities. *Journal of Aerosol Science*, 40(3):256–269, 2009.

[18] L. Morawska, J. W. Tang, W. Bahnfleth, P. M. Bluyssen, A. Boerstra, G. Buonanno, J. Cao, S. Dancer, A. Floto, F. Franchimon, et al. How can airborne transmission of covid-19 indoors be minimised? *Environment International*, page 105832, 2020.

[19] W. W. Nazaroff. Indoor particle dynamics. *Indoor air*, 14(Supplement 7):175–183, 2004.

[20] W. W. Nazaroff. Indoor bioaerosol dynamics. *Indoor Air*, 26(1):61–78, 2016.

[21] Y. Pan, D. Zhang, P. Yang, L. L. Poon, and Q. Wang. Viral load of sars-cov-2 in clinical samples. *The Lancet Infectious Diseases*, 20(4):411–412, 2020.

[22] S. Park, Y. Kim, S. Yi, S. Lee, B. Na, C. Kim, J. Kim, H. Kim, Y. Kim, Y. Park, et al. Coronavirus disease outbreak in call center, south korea. *Emerging infectious diseases*, 26(8), 2020.

[23] E. Riley, G. Murphy, and R. Riley. Airborne spread of measles in a suburban elementary school. *American journal of epidemiology*, 107(5):421–432, 1978.

[24] C. Rothe, M. Schunk, P. Sothmann, G. Bretzel, G. Froeschl, C. Wallrauch, T. Zimmer, V. Thiel, C. Janke, W. Guggemos, et al. Transmission of 2019-ncov infection from an asymptomatic contact in germany. *New England Journal of Medicine*, 382(10):970–971, 2020.

[25] J. L. Santarpia, D. N. Rivera, V. Herrera, M. J. Morwitzer, H. Creager, G. W. Santarpia, K. K. Crown, D. Brett-Major, E. Schnaubelt, M. J. Broadhurst, et al. Aerosol and surface transmission potential of sars-cov-2. *medRxiv*, 2020.

[26] V. Stadnytskyi, C. E. Bax, A. Bax, and P. Anfinrud. The airborne lifetime of small speech droplets and their potential importance in sars-cov-2 transmission. *Proceedings of the National Academy of Sciences*, 117(22):11875–11877, 2020.

[27] G. N. Sze To and C. Y. H. Chao. Review and comparison between the wells–riley and dose-response approaches to risk assessment of infectious respiratory diseases. *Indoor air*, 20(1):2–16, 2010.

[28] R. Tellier, Y. Li, B. J. Cowling, and J. W. Tang. Recognition of aerosol transmission of infectious agents: a commentary. *BMC infectious diseases*, 19(1):101, 2019.

[29] N. Van Doremalen, T. Bushmaker, D. H. Morris, M. G. Holbrook, A. Gamble, B. N. Williamson, A. Tamin, J. L. Harcourt, N. J. Thornburg, S. I. Gerber, et al. Aerosol and surface stability of sars-cov-2 as compared with sars-cov-1. *New England Journal of Medicine*, 382(16):1564–1567, 2020.

[30] V. Vuorinen, M. Aarnio, M. Alava, V. Alopaeus, N. Atanasova, M. Auvinen, N. Balasubramanian, H. Bordbar, P. Erästö, R. Grande, et al. Modelling aerosol transport and virus exposure with numerical simulations in relation to sars-cov-2 transmission by inhalation indoors. *Safety Science*, page 104866, 2020.

[31] L.-s. Wang, Y.-r. Wang, D.-w. Ye, and Q.-q. Liu. A review of the 2019 novel coronavirus (covid-19) based on current evidence. *International journal of antimicrobial agents*, page 105948, 2020.

[32] W. Wells. On air-borne infection: Study ii. droplets and droplet nuclei. *American journal of Epidemiology*, 20(3):611–618, 1934.

[33] Wikipedia contributors. Air changes per hour — Wikipedia, the free encyclopedia, 2020. [Online; accessed 20-June-2020].

[34] R. Wölfel, V. M. Corman, W. Guggemos, M. Seilmaier, S. Zange, M. A. Müller, D. Niemeyer, T. C. Jones, P. Vollmar, C. Rothe, et al. Virological assessment of hospitalized patients with covid-2019. *Nature*, 581(7809):465–469, 2020.

[35] World Health Organization. Transmission of SARS-CoV-2: implications for infection prevention precautions, 2020. [Online; accessed 20-June-2020].

[36] S. Yezli and J. A. Otter. Minimum infective dose of the major human respiratory and enteric viruses transmitted through food and the environment. *Food and Environmental Virology*, 3(1):1–30, 2011.